Physica A 547 (2020) 124475

Contents lists available at ScienceDirect

Physica A

journal homepage: www.elsevier.com/locate/physa

Network properties of healthy and Alzheimer brains

José C.P. Coninck [a], Fabiano A.S. Ferrari [b,*], Adriane S. Reis [c], Kelly C. Iarosz [d], Iberê L. Caldas [d], Antonio M. Batista [d,e], Ricardo L. Viana [c]

[a] Department of Statistics, Technological University of Paraná, 80230-901, Curitiba, PR, Brazil
[b] Institute of Engineering, Science and Technology, Federal University of the Valleys of Jequitinhonha and Mucuri, 39447-790, Janaúba, Brazil
[c] Department of Physics, Federal University of Paraná, 80060-000, Curitiba, PR, Brazil
[d] Institute of Physics, University of São Paulo, 05508-900, São Paulo, SP, Brazil
[e] Department of Mathematics and Statistics, State University of Ponta Grossa, 84030-900, Ponta Grossa, PR, Brazil

ARTICLE INFO

Article history:
Received 14 August 2019
Received in revised form 21 January 2020
Available online 13 March 2020

Keywords:
Network
Human brain
Alzheimer's disease
Small-world

ABSTRACT

The application of graph theory in diffusion weighted resonance magnetic images have allowed the description of the brain as a complex network, often called structural network. For many years, the small-world properties of brain networks have been studied and reported. However, few studies have gone beyond of clustering and characteristic path length. In this work, we compare the structural connection network of a healthy brain and a brain affected by Alzheimer's disease with artificial small-world networks. Based on statistical analysis, we demonstrate how artificial networks can be constructed using Newman–Watts procedure. The network quantifiers of both structural matrices are identified inside a probabilistic valley. Despite of similarities between structural connection matrices and artificial small-world networks, increased assortativity can be found in the Alzheimer brain. Due to limited experimental data, we cannot define a direct link between Alzheimer's disease and assortativity. Nevertheless, we intend to call attention for an important network quantifier that has been neglected. Our results indicate that network quantifiers can be helpful to identify abnormalities in real structural connections, for instance Alzheimer's disease that disrupts the communication among neurons. One of our main results is to show that the network indicators of the Alzheimer brain are almost identical with the small-world network, except the assortativity.

1. Introduction

One of the first fully reported neural network was the worm C. elegans [1]. The nervous system of C. elegans consists of 302 neurons connected through 5000 chemical and 600 electrical synapses. Due to high clustering and short average distance between nodes, Watts and Strogatz suggested that C. Elegans brain network can be considered small-world [2,3]. Small-world networks have been observed in brain networks of animals and humans [4–7]. Evidences of small-world properties can also be found in ensembles of neurons *in vitro* [8]. The smallworldness of neuronal networks is hypothesised to be a consequence of optimisation process associated with minimal wiring cost, robustness and balance between local processing and global integration [9,10].

* Corresponding author.
E-mail address: fabiano.ferrari@ufvjm.edu.br (F.A.S. Ferrari).

https://doi.org/10.1016/j.physa.2020.124475
0378-4371/

Brain networks can be obtained in different levels, such as microscale, mesoscale, and macroscale [11,12]. Microscale is in the level of the neurons and synapses, macroscale is used to define brain regions and large-scale communication pathways. Mesoscale is an intermediate level between micro and macroscale, where connections between large portions of the neuronal system are defined. A simple example of mesoscale network is the mini-columns [13].

Neuronal networks are defined into structural or functional [14]. Functional networks are based on EEG, MEG or fMRI measures [15]. Functional networks of Alzheimer's patients present increased path length when compared with healthy subjects [16].

Structural connections can be characterised by diffusion weighted magnetic resonance imaging (DW-MRI) and graph theory [17]. DW-MRI analyses water diffusion in white matter, and together with fibre tractography it can be used to identify structural connections in the brain [18]. The structural connection matrices of macaque and cats exhibit a complex structure [19]. The presence of clusters and modular architecture in structural connection matrices are observed by means of cortical thickness measurements [20]. Brain networks with small-world properties and exponentially truncated power law distribution were also reported [21].

In humans, the structural connection matrix mediates several complex cognitive functions [22]. Abnormalities in structural networks were found in patients with psychiatric disorders and neurodegenerative diseases [23–26]. Disconnection between frontal and temporal cortices were observed in patients with Schizophrenia [27,28]. Hyperconnectivity in the frontal cortex were reported in patients with Autism [29]. Alzheimer's patient showed increased path length and reduced global efficiency [17]. The alterations in brain networks are good indicators that network properties can be used as biomarkers for clinical applications [30].

Using diffusion tensor tractography, Lo et al. [17] constructed brain networks from experimental data of healthy and Alzheimer's subjects. The network is divided in 78 areas according to the automated anatomic label template [31]. The connection between the areas are defined in terms of the number of fibres, that were obtained through fibre assignment by continuous tracking algorithm [32].

In this work, we analyse the network properties of structural connection matrices of one healthy subject and one subject suffering of Alzheimer's disease. After identifying the network properties, such as, transitivity, path length, assortativity, we demonstrate that similar networks can be constructed using Newman–Watts procedure. One of our main results is to show that the network indicators of the Alzheimer brain are almost identical with the small-world network, except the assortativity.

In Section 2, we provide a brief discussion about the network representation of the connectome. In Section 3, we introduce basic quantities that can be used to quantify networks. In Section 3.2, we demonstrate how to generate a sample of small-world networks with statistical significance. In Section 4, we compare the properties of human brain networks to small-world networks. In Section 5, we present our final remarks.

2. Methodology

Our analysis consist of quantification of network properties, that are going to be discussed in Section 2.1. The procedures to generate a sample of small-world networks with statistical significance are going to be discussed in Section 2.2.

2.1. Properties of networks

Network properties provide information about segregation, integration and influence [33,34]. Segregation properties are associated with the presence of clusters or modules and integration properties are related to the network ability to transmit information through its nodes. Segregation and integration are linked with the network features while influence focus on the node features proving information about the relevance of a node inside the network.

2.1.1. Eigenvalues of the adjacency matrix

The eigenvalues of the adjacency matrix A are obtained by solving the characteristic equation of A,

$$\det(A - \lambda I) = 0, \tag{1}$$

where I is the identity matrix and the values of λ that satisfy Eq. (1) are the eigenvalues [35]. If the network is symmetric, $A_{ij} = A_{ji}$, then all the eigenvalues are real.

2.1.2. Degree and node strength

Degree κ_i is the number of neighbours of a node i,

$$\kappa_i = \sum_{j=1}^{N} A_{ij}, \tag{2}$$

where N is the network size. It is considered one of the simplest measures to provide information about the influence of the network. The degree distribution is used to differentiate regular networks from random networks.

For weighted networks (W_{ij}), the use of node strength s_i instead of degree κ_i may be more appropriated [36]. Node strength s_i is defined as the sum of the node connections,

$$s_i = \sum_{j=1}^{N} W_{ij}. \tag{3}$$

2.1.3. Transitivity

Transitivity T, also known as clustering, is a measure of the segregation of a network. The transitivity T is a measure of the amount of clustering between the node i and its k_i neighbours, the maximum number of connections between i neighbours is $C_{\max(i)} = k_i(k_i - 1)/2$. C_i is defined as the ratio between the number of active connections over the maximum number of connections $C_{\max(i)}$. The transitivity T is the average over all nodes of the network.

The transitivity shows the effective proportion of the triangulation formed between the sites as a measure of clustering capacity, $G(E, V)$. Then, T is calculated by the following proportional ratio

$$T = \frac{3\delta(G)}{\tau(G)}, \tag{4}$$

where $\delta(G)$ is the number of triangles in graph G and $\tau(G)$ denotes the number of triples in graph G [37].

One simple method is to use the arithmetic mean [38]. If the nodes i, j, and k are connected, forming a triplet, the value of the triplet is the arithmetic mean between W_{ij} and W_{jk}. A triplet is considered a close tripled when the nodes i, j, and k are all connected to each other.

2.1.4. Characteristic path length

Characteristic path length L measures the average of the shortest paths d_{ij} between all pairs of nodes in the network,

$$L = \frac{2}{N(N-1)} \sum_{i=1}^{N} \sum_{j=1}^{N} d_{ij}. \tag{5}$$

This quantity is used for weighted and unweighted networks, it provides information about the network integration. When dealing with diffusion process and weighted networks, to calculate the shortest paths d_{ij} the inverse of the node strength should be used [36]. For example, if $W_{12} = 2$, then $d_{ij} = 1/2$, this approach considers that the higher is the node strength the faster information can be diffused through it.

2.1.5. Modularity

Networks can be divided in two or more modules, the trivial solution is to divide them into two modules, where one module has one node and another module containing all the remaining nodes. Basically, the modular structure is defined for any network and the question is to know the best method to identify modules in complex networks. An optimised quantity to characterise the modularity Q was defined by Newman [39], that is given by

$$Q = \frac{1}{4m} \sum_{ij} \left(A_{ij} - \frac{k_i k_j}{2m} \right) (s_i s_j + 1), \tag{6}$$

where $m = 1/2 \sum_i k_i$, s_i, and s_j are indices that depend on the group. The network is divided in two groups, if the site j belongs to group 1, then $s_j = 1$, if j belongs to group 2, then $s_j = -1$. Q can be either positive or negative, positive values indicate the possible presence of community structure.

2.1.6. Assortativity

Assortativity (ASR) is a measure of the tendency of high connected nodes to be connected to others of similar degree k [40]. When high connected nodes are more often connected to low connected nodes, the network exhibits dissortative mixing. To define assortativity it is necessary to define the remaining $q(k)$ and $p(k)$. The probability that a random node has a degree k is given by the degree distribution $p(k)$, however, the probability to select a random edge is not proportional to $p(k)$ but to $kp(k)$, because the most connected nodes receive more connections. Considering that node i is connected to node j through a random selected edge, the remaining degree is the number of nodes that leaves the node j, excluding node i. The normalised remaining degree distribution is given by

$$q(k) = \frac{(k+1)p(k)}{\sum_j jp(j)}. \tag{7}$$

The assortativity ASR is defined as:

$$\mathrm{ASR} = \frac{1}{\sigma_q^2} \sum_{ij} ij(e(i,j) - q(i)q(j)), \tag{8}$$

where σ_q^2 is the variance of the remaining degree and $e(i, j)$ is the joint probability distribution of the remaining degree of two nodes [41]. The assortativity A is defined in the interval $-1 \leq A \leq 1$, when $A = 1$ the network has perfect assortative mixed patterns, $A = 0$ indicates the network is not assortative and $A = -1$ means the network is completely dissortative.

Table 1
Cronbach's alpha.

Alpha	Internal consistency
$0.9 \leq \alpha$	Excellent
$0.8 \leq \alpha \leq 0.9$	Good
$0.7 \leq \alpha \leq 0.8$	Acceptable
$0.6 \leq \alpha \leq 0.7$	Questionable
$0.5 \leq \alpha \leq 0.6$	Poor
$\alpha < 0.5$	Unacceptable

2.2. Statistical analysis

In order to construct a sample of small-world networks we used multivariate data analysis and selected the networks whose networks properties satisfied a set of 34 questions (Table 2).

2.2.1. Multivariate data analysis

Multivariate analysis is a branch of statistics that deals with the relationship between many variables, including the reduction of the number of variables observed during an experiment. The main tools for multivariate data analysis are principal component analysis (PCA) [42], factor analysis [43], classifications [43], structural equations models (SEM) [44,45], among other techniques. In our case, the multivariate analysis of the data is useful to vary the possible second order relationships between variables not directly correlated, such as transitivity, assortativeness and the modularity of the human network. At the end of this paper, we will show how these measures are related using the SEM [45].

2.2.2. Development of a questionnaire

We apply a questionnaire to a population in the small-world models artificially generated with network size in 3 to 100 sites, from a single connection to the global connection. The determination of sample [46]

$$n = \frac{\sum_{N=3}^{100}\sum_{k=1}^{N}\binom{N}{k}\hat{p}\hat{q}z_{\alpha/2}^2}{\hat{p}\hat{q}z_{\alpha/2}^2 + (\sum_{N=3}^{100}\sum_{k=1}^{N}\binom{N}{k} - 1)E^2}, \tag{9}$$

for optimisation $\hat{p} = \hat{q} = \frac{1}{2}$, with error $E \approx \pm 3\%$ in $N = 2499$ population with $z_{\alpha/2}$ is a z-score distribution with level of significance $\alpha \approx 5\%$. In this case, the sample is $n \approx 492$ small-world models. This questionnaire is composed of 34 variables or questions about graph proprieties and applied to each small-world. Each model randomly generated with a certain probability is measured with these thirty-four variables.

We verify the quality of the questionnaire through Cronbach's α [47]

$$\alpha = \frac{K}{K-1}\left(1 - \frac{\sum_i \sigma_{Y_i}^2}{\sigma_{X_i}^2}\right), \tag{10}$$

where K is the number of components, $\sigma_{X_i}^2$ is the variance of the observed total test scores, and $\sigma_{Y_i}^2$ is the variance of the current sample of generated small world. The questionnaire quality (Table 1) applied to small-world networks is equal to 0.89, indicating a good Internal consistency [45,47]. There are different reports about the acceptable values of α. In our study, we use a narrow range of α (Table 1) that is commonly accepted in the literature, mainly for dichotomous or Likert scale questions.

The questionnaire is composed of thirty-four questions (or variables) measured directly in each artificial small-world network, as shown in Table 2. Each variable measures an important network property and the comparison between the human network and the small-world model is given by means of these measures. The small global templates are generated with 10 sites up to 100 sites. Each generated model has different connections of its neighbourhood between a single neighbour and the global network. This way, 492 samples of small-world networks are produced. The measure of sampling adequacy (RMSA) through the Kaiser–Meyer–Olkin (KMO) test indicates considered reasonable for value KMO= 0.73 [48]. The KMO and RMSA measures are given by

$$\text{KMO} = \frac{\sum_{i=1}^{k}\sum_{j=1}^{k} r_{ij}}{\sum_{i=1}^{k}\sum_{j=1}^{k} r_{ij}^2 + a_{ij}^2}, \tag{11}$$

and

$$\text{RMSA} = \frac{\sum_{j=1}^{k} r_{ij}}{\sum_{j=1}^{k} r_{ij}^2 + a_{ij}^2}, \tag{12}$$

where r_{ij} is the correlation matrix term and a_{ij} is the anti-image-correlation matrix term. In this method, the inverse correlation matrix is close to the diagonal matrix. To verifies if matrix correlations is statistical equivalent to an identity

Table 2
Variables of questionnaire - graph.

N	Number of nodes	p	Probability connection
DE	Density edge	L	Average path length
Rep	Reciprocity	E	Edges
N	Vertices	NL	Number of links
NL_l	Internal number of links	DL	link Density
TST	Total System Throughput	TSFR	Total System Flow Rate
Cn	Conectancie	ALW	Average Link Weight
ACT	Average Compartment Throughflow	Cp	Compartmentalisation
T	Transitivity	ASR	Assortativity
Ecc	Eccentricity	D	Diameter
I_{max}	Maximum interweaving	$I_{\min}$	Minimum interweaving
Q	Modularity	E	Efficiency
R	Radius	$K_{\max}$	Max K-Core
$K_{\min}$	Min K-Core	K_{mean}	Mean K-Core
Iso	Isomorfism	Auto	Automorphism
EfcM	Number of edge with max efficiency	Efcm	Number of edge with minimal efficiency
λ_p	Principal eigenvalues	det$M$	Determinant matrix

Table 3
Network indicators (W: Weighted Un: Unweighted).

	Healthy		Alzheimer	
	W	Un	W	Un
Transitivity T	0.578	0.578	0.560	0.559
Assortativity ASR	0.081	0.010	0.226	0.125
Path length L	2.248	2.248	2.281	2.281
Modularity M_1	0.451	0.423	0.483	0.428
σ	23.27	0.590	7.534	0.590
Average degree	8.000	1.383	17.487	1.383

matrix, we use the Bartlett's test. The basic hypothesis is that population's correlation matrix is an identity matrix equivalent. In our variables group, p-value $\ll 0.05$ implies the rejection of the null hypothesis and accepting the factorial analysis.

3. Results

3.1. Structural connection matrices

In this work, we use two structural connection matrices, one for the healthy brain (Fig. 1(a)) and other for the Alzheimer's brain (Fig. 1(b)) [17]. The matrices were obtained by Lo et al. [17], where the nodes of the brain networks were determined through automated anatomical labelling template. They used diffusion magnetic resonance imaging tractography methods and fibre assignment by continuous tracking algorithm to determine the edges and the number of fibres, respectively. According to the number of fibres, we define the weight values, that are distributed by the frequency of the interconnected fibre. Both networks are weighted and symmetric, the weight is associated with the intensity of connections and can assume four values: 0 (no connections, white region), 1 (low density of connections, indigo circles), 2 (intermediate density of connections, red circles), and 3 (high density of connections, orange circles). The main results for the networks are shown in Table 3. Fig. 1 exhibits two adjacency matrix connection W_{ij}: (a) healthy brain and (b) Alzheimer's brain. The eigenvalues for these adjacency matrix are evaluated in Fig. 2. The healthy structural connection matrix is in black and Alzheimer's structural connection matrix is in red. The eigenvalue spectrum for small world with 78 nodes is $p = 0.0375$ (blue line). The ordinate eigenvalues are very close for three structures matrix. The eigenvalues are equivalent when there is some difference in the dispersion of adjacency matrix.

3.2. Small-world networks

The small-world networks have not only a high clustering coefficient (like regular graphs), but also a high average shortest path length (like random graphs) [2]. Many real world networks exhibits small-world property, such as social [49], technological [50], and biological [5] networks. One phenomenon that has been observed in small-world networks is the synchronisation, for instance synchronous behaviour in coupled oscillators [51] and clustered network of neurons [52].

A network with small-world properties can be generated by means of different methods [53]. The most common method was developed by Watts and Strogatz [53], where the regular edges are replaced by random edges. When about 1% of the total edges are replaced, the network exhibits high transitivity and low path length [2]. For our analysis, we consider an alternative method, where instead of randomly replace regular edges by random edges, we only add random

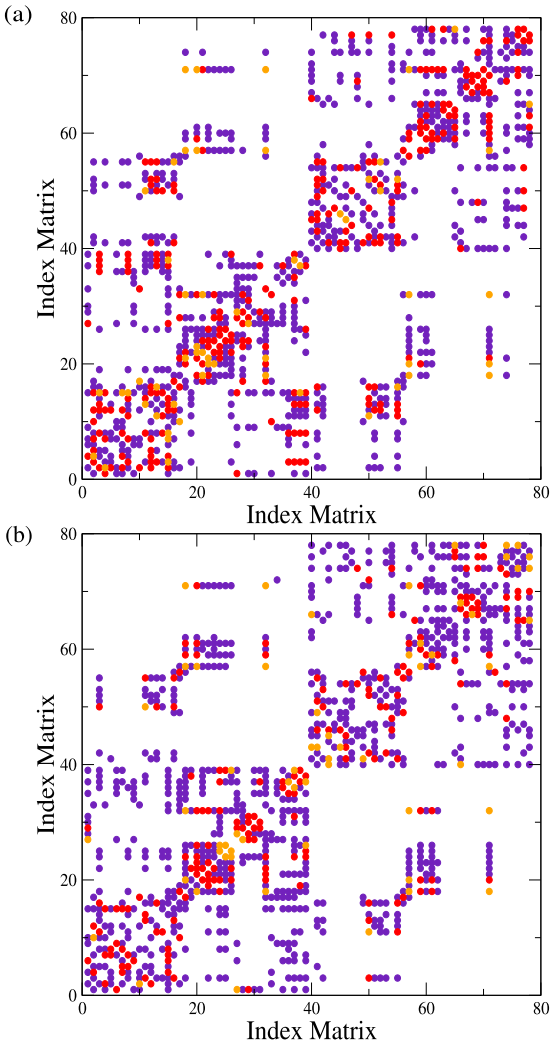

Fig. 1. Weighted connection matrix W_{ij} for (a) healthy and (b) Alzheimer's brains. The weight is associated with the intensity of connections: 0 (no connections, white region), 1 (low density of connections, indigo circles), 2 (intermediate density of connections, red circles), and 3 (high density of connections, orange circles).

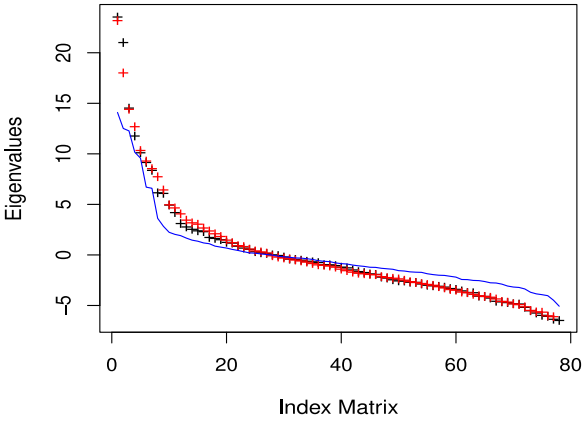

Fig. 2. Eigenvalue spectrum for the weighted matrices of Fig. 1. Healthy structural connection matrix is in black and Alzheimer's structural connection matrix is in red. Eigenvalue spectrum for small-world with 78 nodes and connection probability is $p = 0.0375$ in blue continue line.

Table 4
Transitivity loss (weighted).

	Healthy	Alzheimer	Loss
Transitivity	0.57813	0.5598876	3.1%
Nodes	78	78	
Links total	1040	1044	
Transfer rate	1438	1364	5.4%
Leak rate	1438	1364	5.4%

edges, known as Newman–Watts procedure [54]. We add pNK new random edges, where N is the network size, K is the regular network degree, and p is the probability to add new edges. We vary p and identify the small-world properties comparing T and L with the values of the regular network $T(0)$ and $L(0)$. We find

- Healthy brain

$$\text{DL: link density} \longrightarrow \frac{DL}{2} = \frac{13.3333}{2} \approx 7, \tag{13}$$

- Alzheimer's brain

$$\text{DL: link density} \longrightarrow \frac{DL}{2} = \frac{13.38462}{2} \approx 7. \tag{14}$$

The number of nodes in the human graph is 78 sites and the average degree is 7 neighbours per node. Due to this fact we create the equivalent connection network under these conditions to depend exclusively on the probability of calling. It is generated small-world graph with number of nodes $N = 78$, 7 neighbours per node, and without the likelihood of connection ($p = 0$), implying in average length $L_0 = 3.27273$ and transitivity $C_0 = 0.69231$. For both networks of Fig. 1

$$\frac{C}{C_0} > \frac{L}{L_0}. \tag{15}$$

For healthy brain, we find $L_{\text{healthy human}} = 2.24875$ and $C_{\text{healthy human}} = 0.57813$. C/C_0 is approximately 1.4% more than Alzheimer's brain, and L/L_0 is approximately 3.1% less than Alzheimer's brain. The propagated information in Alzheimer's network presents greater difficulty for diffusion of information in network, becoming more complex than healthy human matrix. Therefore, there seems to be a relationship between the transfer of the network and its grouping, i.e., relations between assortivity, modularity and transitivity.

3.2.1. Regression analysis

In a convenience sample, for $n = 429$ small-world type networks, five replicas are executed to create variation within the others. The dispersion of the transitivity according to the logarithm of the connection probability shows a decay adjusted by generalised model Gaussian family with link identity

$$f(y|\mu, \sigma^2) = \exp\left[\frac{1}{\sigma^2}\left(y\mu - \frac{\mu^2}{2}\right) + \left(-\frac{1}{2}\ln(2\pi\sigma^2) - \frac{y^2}{2\sigma^2}\right)\right], \tag{16}$$

resulting in the following regression

$$T_{\text{SW}} = 0.300314 - 0.029338 \ln p. \tag{17}$$

For instance, when the probability connection is $p = 9.1188196 \times 10^{-4}$, then $\log p$ is equal to -7 and T_{SW} is approximately 0.50568. This probability value p is in agreement with the probability of small-world connection. When the connection probability increases, the dispersion of the transitivity value increases as well. On the other hand, the decrease in probability linkage causes the dispersion to become smaller and more concentrated, characterising a good small-world region. $T_{\text{H}} = T_{\text{M}} = T_{\text{SW}}$ is valid for the small-world model. Another feature of Eq. (17) is its rate of transitivity in relation to the log of the probability,

$$\frac{dT_{\text{SW}}}{d\ln p} = -0.029338 \approx -3\%. \tag{18}$$

The ratio of transitivity to $\ln p$ is equal to the loss value in the small-world model when we compare the matrix of healthy human adjacency with disease Alzheimer human matrix.

The transfer rate and the rate of flow in the network with Alzheimer's exhibit a drop equal to that caused in the transitivity when compared with the human network in the normal state, as shown in Table 4. It suggests that the rate of transfer and rate of flow for people with Alzheimer's disease declines with 5.4%, possibly due to the fall in transitivity in 3.1%.

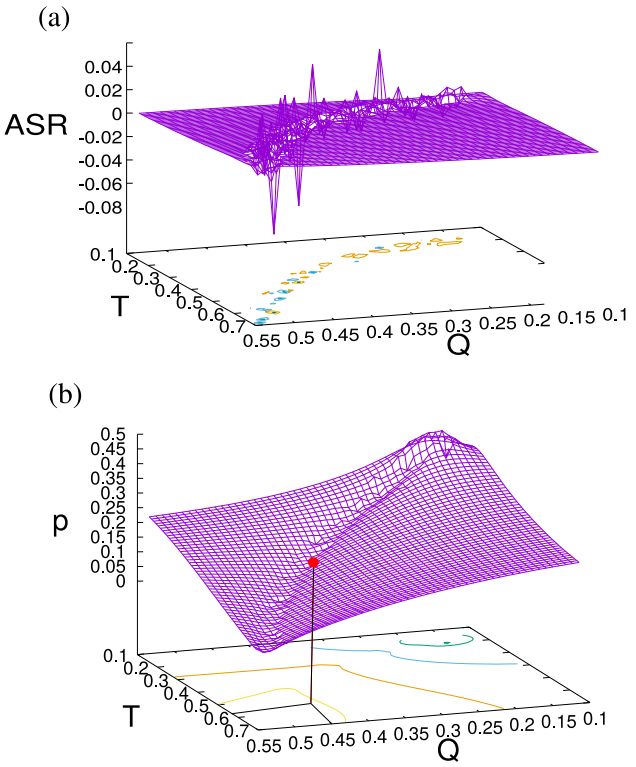

Fig. 3. Probabilistic valley as functions of modularity (Q) and transitivity (T) for:(a) Assortativity and (b) probability of non-local connections. The red dot is located in the region where the modularity (≈ 0.45) and transitivity (≈ 0.58) have values approximately equal to the healthy brain. In addition, it coincides with the result of the assortativity (≈ -0.02) in the Alzheimer's brain.

3.2.2. Assortativity

One of the most difficult measure to be statistically analysed is the assortativity of the network. Due to the fact that the network topology of small-world is very sensitive to the probability of (re)connection. This can be verified in healthy and Alzheimer's networks. For $T = 0.57$, the values of assortativity show huge variation. However, the assortativity of the Alzheimer's brain is 2.5 times higher than for healthy brain (Table 3).

We calculate the assortativity distribution for small-world networks for $n = 492$ samples. In a sample, for example $N = 10$ and second order connection, the assortativeness presents $< \text{ASR} >= -0.01335938$ that is not statistically zero according to t-Student test for the hypothesis $H_0 : \mu_{\text{ASR}} = 0$. There is no significant evidence supporting the null hypothesis for a p-value $\ll 0.05$, inclining us to accept the hypothesis that the assortativeness in the sample question is, in fact, negative. This does not imply the formation of positive assortativeness as verified in the graph.

3.2.3. Probabilistic valley

The probabilistic valley is a region where the small-world structure behaves by sequences of abrupt changes. It is precisely in this region that we identify abrupt behaviour of assortativeness, given the equivalent modularity and transitivity. These three measures of the small-world model that are equivalent to the measurements of the human matrix are found in this valley. The probabilistic voucher is developed through the structural equations model (SEM), in which it is related indirectly to assortativity, transitivity and modularity. As assortativeness represents the equivalent of the correlation between the links of the sites of a network, we write the assortativity in function of the transitivity and the modularity of the network for determinate probabilistic valley.

The probabilistic valley region indicates a possible existence of probability as a function of the modularity, transitivity and efficiency, that it is in agreement with the SEM analysis. This indicates that there is a possible dependence on the functions of modularity, assortativeness, transitivity and efficiency, according to the SEM analysis. In the same region random overflow occurs in assortativity increasing transitivity and modularity. The increase in assortativity and transitivity implies in the decay of the connection probability, which confirms that the probability value decreases. A more detailed view of the level curve with the modularity in the abscissa of the assortative at the ordinate reveals a complex structure of the curves. Outside this region the value of the assortativeness is zero or close to zero.

The valley has many interesting behaviour. To generate Fig. 3, we consider a set of 100 independent models of small-world networks starting with 10 sites up to the amount 100 sites. In all models, we vary the probability of linkage between

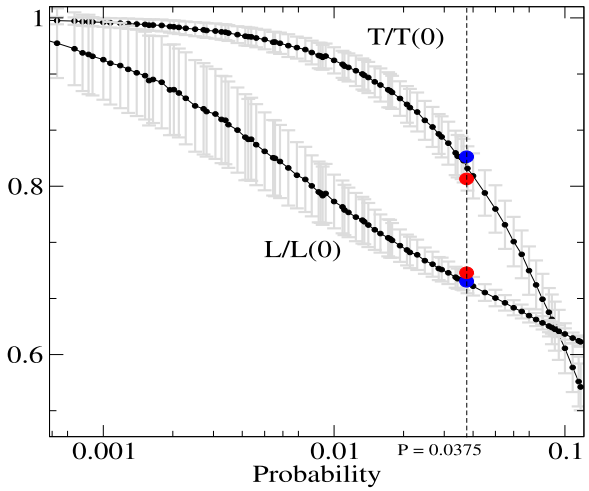

Fig. 4. Relative values of path length $L/L(0)$ and transitivity $T/T(0)$ as a function of the probability. The results for healthy and Alzheimer's networks are shown by blue and red dots, respectively. $L(0)$ and $T(0)$ correspond to the values of the path length and transitivity values for the regular network ($p = 0$).

Table 5
Values of the healthy brain and small-world network.

	Health human (real)	Small-world (Simulated)	Error (ε)
Average path length	2.2487	2.1964	+2.32%
Density of links	13.333	14.000	−5.00%
Transitivity	0.5781	0.5386	+6.79%
Assortivity	0.0815	0.0882	−8.32%
Eccentricity	3.6667	3.5128	+4.20%
Modularity	0.4515	0.4889	−8.27%

the non-coupling state ($p = 10^{-6}$) and the overall state ($p = 1$). The red dot in Fig. 3 is located in the region where the modularity (≈ 0.45) and transitivity (≈ 0.58) have values equal to the results found in the healthy brain. The same point coincides with the result of the assortativity (≈ -0.02) in the Alzheimer's brain. This graph located in this point has 78 sites with 7 connections neighbours and probability range $8.10^{-8} < p < 0.5$.

4. Discussion

When we compare the values of the network quantifiers (transitivity, assortativity, modularity, ...) of the brain networks and the small-world samples, we observe they are located in the probabilistic valley. The characteristic path length and transitivity of the small-world samples are presented in Fig. 4. The agreement between the samples and the brain networks occurs at $p = 0.0375$ and it can be observed by the blue and red dots in the figure. Comparing healthy and Alzheimer's networks, we found a difference of 3.1% for transitivity. Transitivity is greater for healthy than Alzheimer's brain, while characteristic path length (L) is the opposite.

The weighted connection matrix eigenvalues W_{ij} is useful for the comparison between the matrix structures. In Fig. 2, we display the eigenvalue spectrum for both networks of Fig. 1. We verify that the eigenvalues of both networks are similar. The eigenvalues of the small-world samples are very close to the human networks.

Table 5 shows that the average path length of the healthy brain is very close to small-world network. The transitivity , assortativity, eccentricity, and modularity are almost identical. In Table 6, we see that the Alzheimer's brain and small-world network have similar values, except the assortativity value, $\varepsilon = 59.62\%$. The positive transitivity is in accordance with previous works [55]. The huge difference in the assortativity was unexpected. However, in functional networks, increased assortativity was observed in patients with clinical dementia rating level 1 [56]. In structural networks, the increased assortativity was reported in patients suffering of Alzheimer's disease with mild cognitive impairment [57].

5. Conclusions

In this work, we show that small-world networks can be used to mimic healthy brain networks. In our case, the healthy brain can be reproduced by a Newman–Watts small-world network of $p = 0.0375$. For average path length, for example, the agreement is 97%.

Table 6
Values of the Alzheimer's brain and small-world network.

	Alzheimer's brain (real)	Small-world (Simulated)	Error (ε)
Average path length	2.28172	2.1964	+3.74%
Density of links	13.3846	14.000	−4.59%
Transitivity	0.55989	0.5386	+3.80%
Assortivity	0.21846	0.0882	+59.62%
Eccentricity	3.76923	3.5128	+6.80%
Modularity	0.49083	0.4889	+0.39%

We find a relation of construction among the variables associated with the transmission of information in the network, such as the transitivity (0.57813 for the healthy brain and 0.5386 for the small-world network), the assortativity (0.08151 for the healthy brain and 0.08829 for the small-world network), the eccentricity (3.66667 for the healthy brain and 3.51282 for the small-world network), and the modularity (0.45157 for the healthy brain and 0.48891 for the small-world network), whose values are very close to each other. In all four measures, we obtained errors (ε) smaller than 10% in the measurements up or down. Both healthy and Alzheimer's networks were within the simulated region for a small-world sample, indicating a close linkage probability of 3.75%. A small-world model in this region, for an equivalent assertiveness value, has very similar graph properties. Therefore, the human network (diseased or not) behaves as a small-world network.

We verify that the healthy brain can be mimicked by networks with small-world properties. The network indicators of the Alzheimer's brain are almost identical with the small-world network, except the assortativity. Despite of our limited set of data, we believe that assortativity can be associated with important changes in structural connections of the brain of Alzheimer's patients.

We have focused in the network composition differences between a normal person and another with Alzheimer. However, a statistical verification should be considered to validate our present conjecture. Here we only use one patient sample, at clinical level, on the other hand, lots of patient samples are required to conclude one indicator for a disease. Due to this fact, in future works, we plan to analyse the network properties of structural connection matrices considering a larger sample of healthy patients and patients suffering of Alzheimer's disease.

Declaration of competing interest

The authors declare that they have no known competing financial interests or personal relationships that could have appeared to influence the work reported in this paper.

Acknowledgements

We wish to thank the Brazilian government agencies: Araucária Foundation, National Council for Scientific and Technological Development, Brazil (CNPq processes: 420699/2018-0 and 407543/2018-0), Coordination for the Improvement of Higher Education Personnel (CAPES), Brazil, and São Paulo Research Foundation, Brazil (Processes 2015/07311-7 and 2018/03211-6). The authors would like to thank the 105 Group Science (www.105groupscience.com) for the fruitful discussions and the Taiwan data results that were supported by Taiwan MOST grants and collected in National Yang-Ming University.

References

[1] J.G. White, E. Southgate, J.N. Thomson, S. Brenner, The structure of the nervous system of the nematode Caenorhabditis Elegans, Philos. Trans. R. Trans. R. Soc. Lond. B 314 (1986) 1–340.
[2] D.J. Watts, S.H. Strogatz, Collective dynamics of 'small-world' networks, Nature 393 (1998) 440–442.
[3] L.R. Varshney, B.L. Chen, E. Paniagua, D.H. Hall, D.B. Chklovskii, Structural properties of the Caenorhabditis Elegans neuronal network, PLOS Comput. Biol. 7 (2011) e100106.
[4] O. Sporns, J.D. Zwi, The small world of the cerebral cortex, Neuroinformatics 2 (2004) 145–162.
[5] D.S. Bassett, E. Bullmore, Small-world brain networks, Neuroscientist 12 (2006) 512–523.
[6] C.J. Stam, Modern network science of neurological disorders, Nat. Rev. Neurosci. 15 (2014) 683–695.
[7] Y. Iturria-Medina, R.C. Sotero, E.J. Canales-Rodríguez, Y. Alemán-Gómez, L. Melie-García, Studying the human brain anatomical network via diffusion-weighted MRI and Graph Theory, Neuroimage 40 (2008) 1064–1076.
[8] L.M.A. Bettencourt, G.J. Stephens, M.I. Ham, G.W. Gross, Functional structure of cortical neuronal networks grown in vitro, Phys. Rev. E 75 (2007) 021915.
[9] J.C. Reijneveld, S.C. Ponten, H.W. Berendse, C.J. Stam, The application of graph theoretical analysis to complex networks in the brain, Clin. Neurophysiol. 118 (2007) 2317–2331.
[10] E. Bullmore, O. Sporns, The economy of brain network organization, Nat. Rev. Neurosci. 13 (2012) 336–349.
[11] O. Sporns, G. Tononi, R. Kötter, The human connectome: A structural description of the human brain, PLOS Comput. Biol. 1 (2005) e42.
[12] M.P. van den Heuvel, B.T.T. Yeo, A spotlight on bridging microscale and macroscale human brain architecture, Neuron 93 (2017) 1248–1251.

[13] R. Stoop, V. Saase, C. Wagner, B. Stoop, R. Stoop, Beyond scale-free small-world networks: Cortical columns for quick brains, Phys. Rev. Lett. 110 (2013) 108105.
[14] E.T. Bullmore, D.S. Bassett, Brain graphs: graphical models of the human brain connectome, Annu. Rev. Clin. Psychol. 7 (2011) 113–140.
[15] C.J. Stam, E.C. van Straaten, The organization of physiological brain networks, Clin. Neurophysiol. 123 (2012) 1067–1087.
[16] C.J. Stam, B.F. Jones, G. Nolte, M. Breakspear, P. Scheltens, Small-world networks and functional connectivity in Alzheimer's Disease, Cereb. Cortex 17 (2007) 92–99.
[17] C.Y. Lo, P.N. Wang, K.H. Chou, J. Wang, Y. He, C.P. Lin, Diffusion tensor tractography reveals abnormal topological organization in structural cortical networks in Alzheimer's disease, J. Neurosci. 30 (2010) 16876–16885.
[18] Y. Iturria-Medina, E.J. Canales-Rodríguez, L. Melie-García, P.A. Valdés-Her-nández, E. Martínez-Montes, Y. Alemán-Gómez, J.M. Sánchez-Bornot, Characterizing brain anatomical connections using diffusion weighted MRI and graph theory, Neuroimage 36 (2007) 645–660.
[19] C.C. Hilgetag, G.A. Burns, M.A. O'Neil, J.W. Scannell, M.P. Young, Anatomical connectivity defines the organization of clusters of cortical areas in the macaque monkey and the cat, Philos. Trans. R. Soc. Lond. B 355 (2000) 91–110.
[20] Z. Chen, Y. He, P. Rosa-Neto, J. Germann, A.C. Evans, Revealing modular architecture of human brain structural networks by using cortical thickness from MRI, Cereb. Cortex 18 (2008) 2374–2381.
[21] G. Gone, Y. He, L. Conhca, C. Lebel, D.W. Grossa, A.C. Evans, C. Beaulieu, Mapping anatomical connectivity patterns of human cerebral cortex using in vivo diffusion tensor imaging tractography, Cereb. Cortex 19 (2009) 524–536.
[22] S.L. Bressler, Large-scale cortical networks and cognition, Brain Res. Rev. 20 (1995) 288–304.
[23] Y. He, Z. Chen, A. Evans, Structural insights into Aberrant Topological patterns of large-scale cortical networks in Alzheimer's Disease, J. Neurosci. 28 (2008) 4756–4766.
[24] Y. He, A. Dagher, Z. Chen, A. Charil, A. Zijdenbos, K. Worsley, A. Evans, Impaired small-world efficiency in structural cortical networks in multiple sclerosis associated with white matter lesion load, Brain 132 (2009) 3366–3379.
[25] Z. Yao, Y. Zhang, L. Lin, Y. Zhou, C. Xu, T. Jiang, Abnormal cortical networks in mild cognitive impairment and Alzheimer's Disease, PLOS Comput. Biol. 6 (2010) e1001006.
[26] H.H. Pol, E. Bullmore, Neural networks in psychiatry, Eur. Neuropsychopharmacol. 23 (2013) 1–6.
[27] K.J. Friston, C.D. Frith, Schizophrenia: a disconnection syndrome? Clin. Neurosci. 3 (1995) 89–97.
[28] A. Zalesky, A. Fornito, M.L. Seal, L. Cocchi, C.F. Westin, E.T. Bullmore, G.F. Egan, C. Pantelis, Disrupted Axonal Fiber connectivity in Schizophrenia, Biol. Psychiatry 69 (2011) 80–89.
[29] E. Courchesne, K. Pierce, Why the frontal cortex in autism might be talking only to itself: local over-connectivity but long-distance disconnection, Curr. Opin. Neurobiol. 15 (2005) 225–230.
[30] M. Kaiser, A tutorial in connectome analysis: Topological and spatial features of brain networks, NeuroImage 57 (2011) 892–907.
[31] N. Tzourio-Mazoyer, B. Landeau, D. Papathanassiou, F. Crivello, O. Etard, N. Delcroix, B. Mazoyer, M. Joliot, Automated anatomical labeling of activations in SPM using a macroscopic anatomical parcellation of the MNI MRI single-subject brain, Neuroimage 15 (2002) 273–289.
[32] S. Mori, B.J. Crain, V.P. Chacko, P.C.van. Zijl, Three-dimensional tracking of axonal projections in the brain by magnetic resonance imaging, Ann. Neurol. 45 (1999) 265–269.
[33] M. Rubinov, O. Sporns, Complex network measures of brain connectivity: uses and interpretations, Neuroimage 52 (2010) 1059–1069.
[34] O. Sporns, Structure and function of complex brain networks, Dialogues Clin. Neurosci. 15 (2013) 247–262.
[35] D. Cvetković, P. Rowlinson, S. Simić, Eigenspaces of Graphs, Cambridge University Press, Cambridge, 1997.
[36] T. Opsahl, F. Agneessens, J. Skvoretz, Node centrality in weighted networks: Generalizing degree and shortest paths, Soc. Netw. 32 (2010) 245–251.
[37] T. Schank, D. Wagner, Approximating clustering-coefficient and transitivity, J. Graph Algorithms Appl. 9 (2005) 265–275.
[38] T. Opsahl, P. Panzarasa, Clustering in weighted networks, Soc. Netw. 31 (2009) 155–163.
[39] M.E.J. Newman, Modularity and community structure in networks, Proc. Natl. Acad. Sci. USA 103 (2006) 8577–8582.
[40] J.G. Foster, D.V. Foster, P. Grassberger, M. Paczuski, Edge direction and the structure of networks, Proc. Natl. Acad. Sci. USA 107 (2010) 10815–10820.
[41] M.E.J. Newman, Assortative mixing in networks, Phys. Rev. Lett. 89 (2002) 208701.
[42] V. Gray, Principal Component Analysis: Methods, Applications, and Technology, Nova Science Publishers, Inc., (Mathematics Research Developments), Hauppauge, New York, 2017.
[43] R.A. Jhonson, D.W. Wischern, Applied Multivariate Statistical Analysis, fourth ed., Pretice Hall, Upper Saddle River, New Jersey, ISBN: 0-13-834194-X, 1998.
[44] J.B. Grace, Structural Equation Modeling and Natural Systems, Cambridge University Press, Cambridge, UK, 2006.
[45] G. Maruyama, Basics of Structural Equation Modeling, SAGE Publications, Inc., Thousand Oaks, Calif., 1998.
[46] W.G. Cochran, Sampling Techniques, John Wiley & Sons, 1977, ISBN-10, 047116240.X.
[47] L.J. Cronbach, Psychometrika 16 (297) (1951) http://dx.doi.org/10.1007/BF02310555.
[48] H.F. Kaiser, Psychometrika 39 (1974) 31, http://dx.doi.org/10.1007/BF02291575.
[49] G. Abramson, M. Kuperman, Social games in a social network, Phys. Rev. E 63 (2001) 030901.
[50] R.F. Cancho, C. Janssen, R.V. Solé, Topology of technology graphs: Small world patterns in electronic circuits, Phys. Rev. E 64 (2001) 046119.
[51] Y. Wu, Y. Shang, M. Chen, C. Zhou, J. Kurths, Synchronization in small-world networks, Chaos 18 (2008) 037111.
[52] E.L. Lameu, F.S. Borges, R.R. Borges, K.C. Iarosz, I.L. Caldas, A.M. Batista, R.L. Viana, J. Kurths, Suppression of phase synchronisation in network based on cat's brain, Chaos 26 (2016) 043107.
[53] M.E.J. Newman, Models of the small world, J. Stat. Phys. 101 (2000) 819–841.
[54] M.E.J. Newman, The structure and function of complex networks, SIAM Rev. 45 (2003) 167–256.
[55] H. Kim, K. Yoo, D.L. Na, S.W. Seo, J. Jeong, Y. Jeong, Non-monotonic reorganization of brain networks with alzheimer's disease progression, Front. Aging Neurosci. 7 (111) (2015).
[56] S. Lim, F. Radicchi, M.P. Heuvel, O. Sporns, Discordant attributes of structural and functional brain connectivity in a two-layer multiplex network, Sci. Rep. 9 (2019) 2885.
[57] S. Galantucci, F. Agosta, E. Stefanova, S. Basaia, M.P. Heuvel, T. Stojković, E. Canu, I. Stanković, V. Spica, M. Copetti, D. Gagliardi, V.S. Kostić, M. Filippi, Structural brain connectome and cognitive impairment in parkinson disease, Radiology 283 (2017) 515–525.